Electronic Supplementary Material (ESI) for RSC Advances.

Supporting information

Enhanced electrocatalytic oxygen redox reactions of iron oxide nanorod films by combining oxygen vacancy formation and cobalt doping

Saleh Omar ben Gubaer,[a,1] Maged N. Shaddad,[b,1] Prabhakarn Arunachalam,[a*] Mabrook S Amer,[a,] [c] Saba A. Aladeemy,[b] Abdullah M Al-Mayouf [a,c,*]

[a]Electrochemical Sciences Research Chair (ESRC), Chemistry Department, College of Science, King Saud University, Riyadh 11451, Saudi Arabia.

[b]Department of Chemistry, College of Science and Humanities in Al-Kharj, Prince Sattam Bin Abdulaziz University, P.O. Box 173, Al-Kharj 11942, Saudi Arabia.

[c]K.A.CARE Energy Research and Innovation Center at Riyadh, 11454, Saudi Arabia.

Corresponding authors

*parunachalam@ksu.edu.sa (P. Arunachalam), amayouf@ksu.edu.sa (A. M.Al-Mayouf), Tel:+96614675959 Fax:+96614675992

[1]These authors contributed equally to this work.

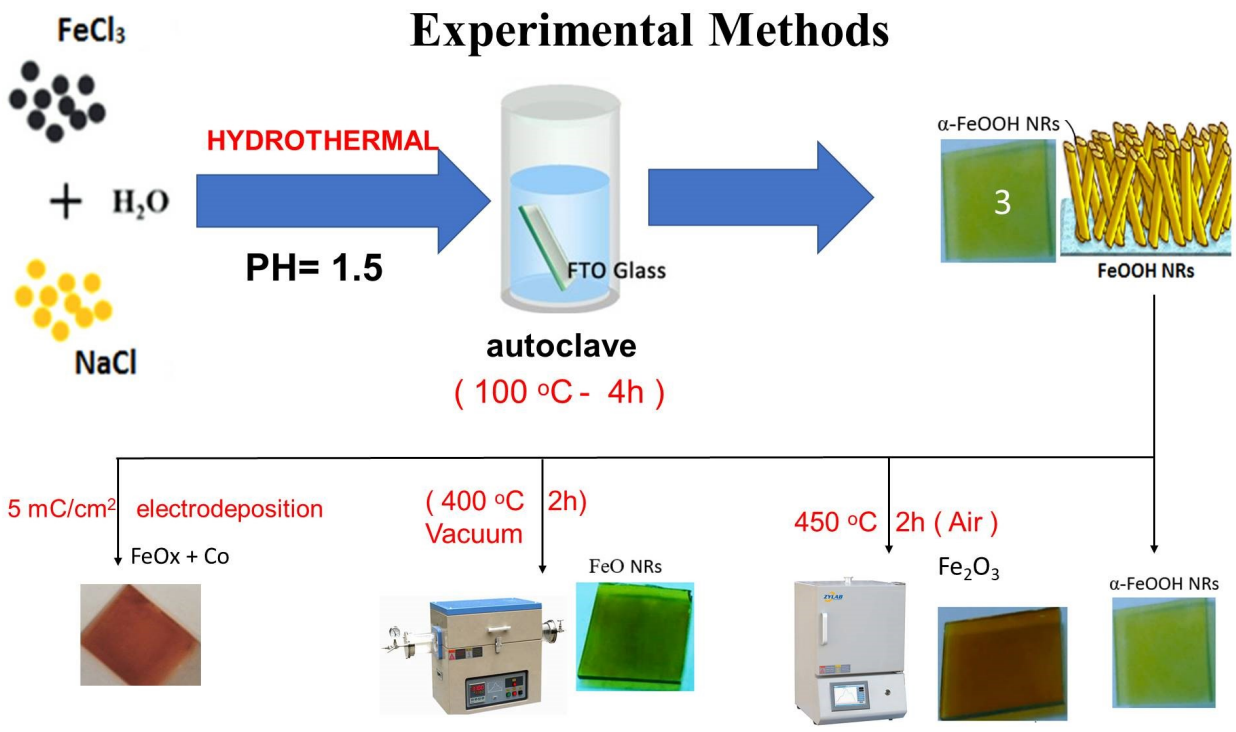

Figure S1. Schematic illustration of the synthesis procedures of fabricated α-FeOOH, Fe_2O_3, FeO, and Co-doped FeO NRs materials.

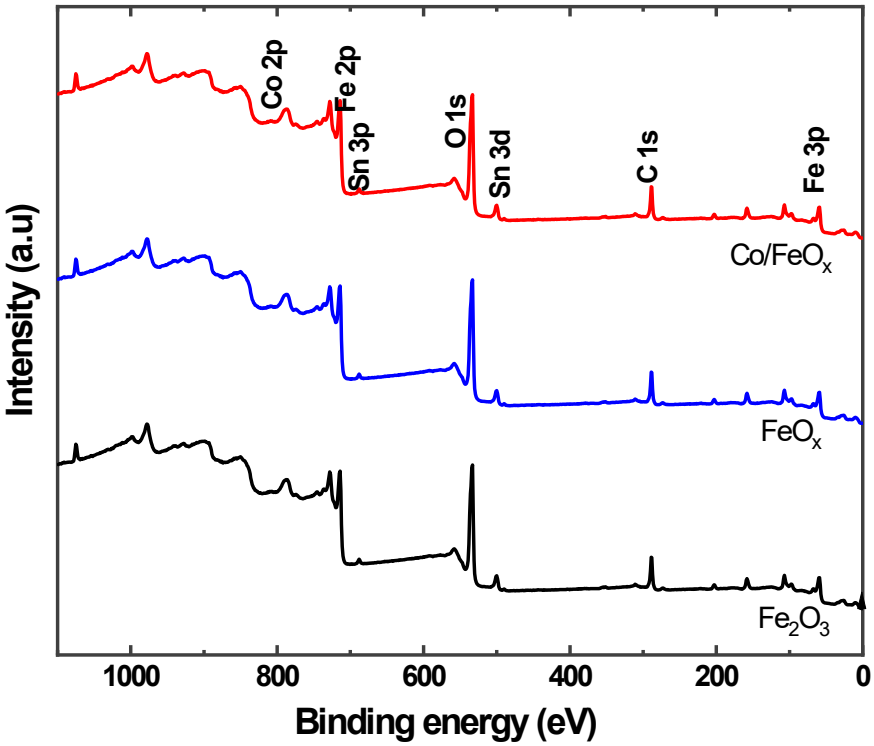

Figure S2. Comparative XPS survey spectra of fabricated Fe_2O_3, FeOx, and Co-doepd FeOx electrodes fabricated by hydrothermal and electrodeposition approaches

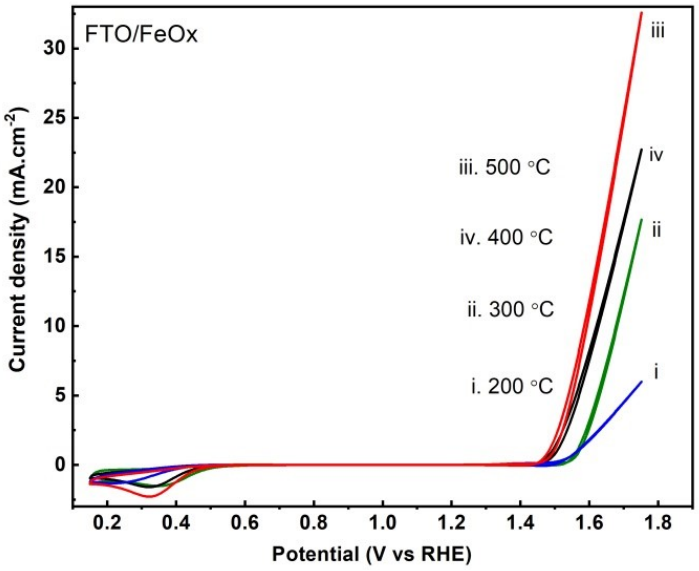

Figure S3. Cyclic voltammetric plots FeO_x/FTO electrode after annealing under Vacuum at different annealing temperatures (in 1.0 M KOH (pH 13.6) with scan rate 10 mVs^{-1}

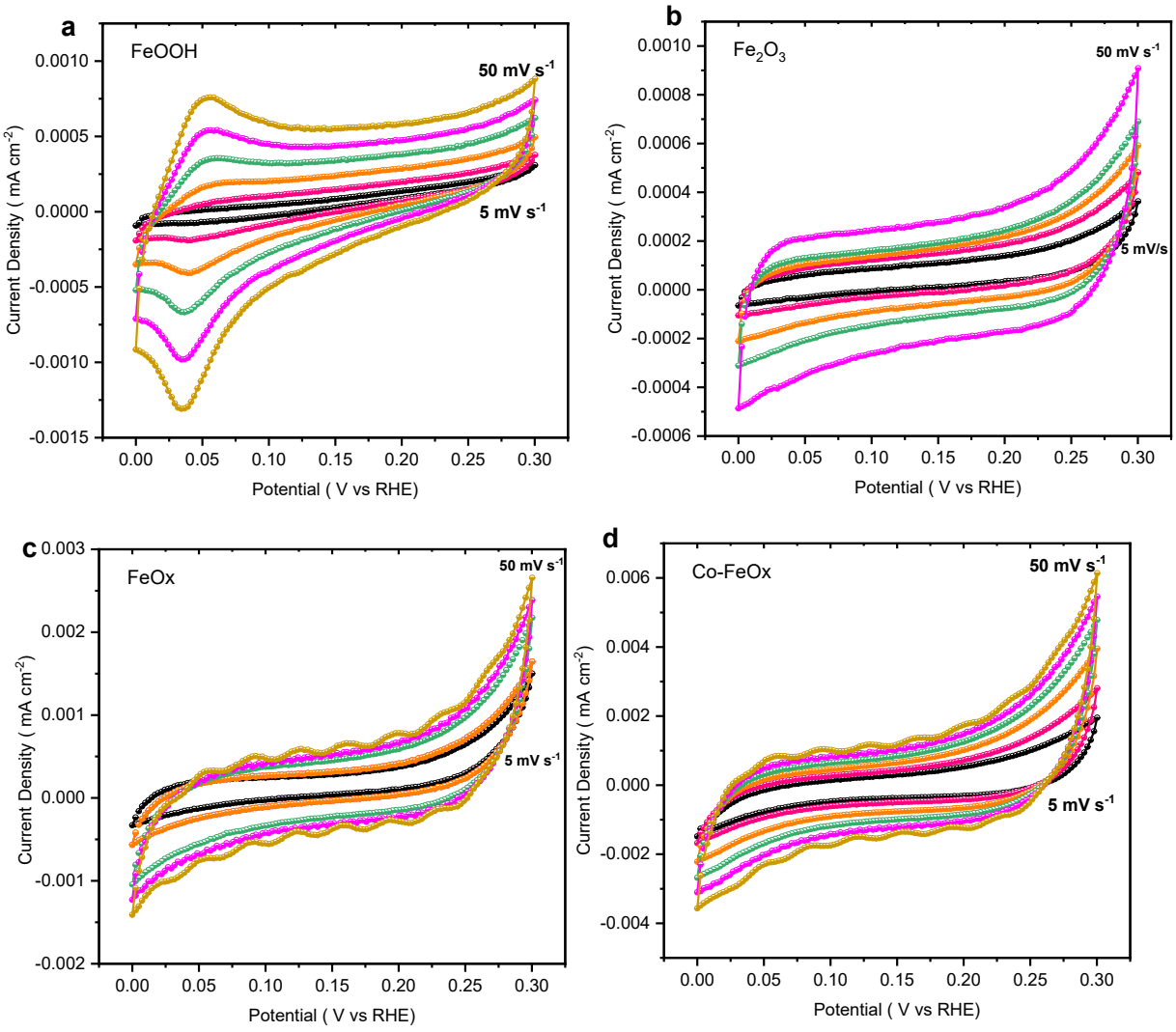

Figure S4. **Electrochemical surface area measurements**. Cyclic voltammograms of a) FeOOH, Fe_2O_3 (b), FeOx (c), Co-doped FeOx (d) electrodes at various scan rates.

Table S1. Impedance parameter values derived from the fitting to the equivalent circuit for the impedance spectra recorded in 1.0 M KOH solution with an applid potential of 1.6 V vs RHE. Rs = solution resistance, Rct = charge-transfer resistance,.

Materials	Rs, Ω	CPE, μMho	Rct, Ω	n
Fe_2O_3 NRs	35	6.02	55.6	0.587
α-FeOOH NRs	21	88.2	17.9	0.764
FeOx NRs	17.5	2.84	6.65	0.700
Co/FeO_x NRs	11.5	10.4	2.61	0.65